Evaluating seismic liquefaction potential using multivariate adaptive regression splines and logistic regression

Wengang Zhang [1,2,3a] and Anthony T.C. Goh[*3]

[1] *Key Laboratory of New Technology for Construction of Cities in Mountain Area, Chongqing University, Ministry of Education, Chongqing 400045, China*
[2] *School of Civil Engineering, Chongqing University, Chongqing 400045, China*
[3] *School of Civil and Environmental Engineering, Nanyang Technological University, 639798 Singapore*

Abstract. Simplified techniques based on in situ testing methods are commonly used to assess seismic liquefaction potential. Many of these simplified methods were developed by analyzing liquefaction case histories from which the liquefaction boundary (limit state) separating two categories (the occurrence or non-occurrence of liquefaction) is determined. As the liquefaction classification problem is highly nonlinear in nature, it is difficult to develop a comprehensive model using conventional modeling techniques that take into consideration all the independent variables, such as the seismic and soil properties. In this study, a modification of the Multivariate Adaptive Regression Splines (MARS) approach based on Logistic Regression (LR) LR_MARS is used to evaluate seismic liquefaction potential based on actual field records. Three different LR_MARS models were used to analyze three different field liquefaction databases and the results are compared with the neural network approaches. The developed spline functions and the limit state functions obtained reveal that the LR_MARS models can capture and describe the intrinsic, complex relationship between seismic parameters, soil parameters, and the liquefaction potential without having to make any assumptions about the underlying relationship between the various variables. Considering its computational efficiency, simplicity of interpretation, predictive accuracy, its data-driven and adaptive nature and its ability to map the interaction between variables, the use of LR_MARS model in assessing seismic liquefaction potential is promising.

Keywords: multivariate adaptive regression splines; logistic regression; seismic liquefaction potential; interaction; basis function; limit state function

1. Introduction

Evaluation of seismic liquefaction of soils can be performed through laboratory tests or numerical simulations (Toyota *et al*. 2004, Lancelot *et al*. 2004, Atigh and Byrne 2004, Lade and Yamamuro 2011, Liu *et al*. 2014, Duman *et al*. 2014, Chen *et al*. 2013, 2015). As an alternative, simplified techniques based on an in situ testing measurement index are commonly used to assess seismic liquefaction potential. Most of these simplified charts or equations rely on the analysis of liquefaction case histories. Using empirical, simple regression, or statistical methods, a boundary

---

(liquefaction curve) or classification technique is used to separate the occurrence or non-occurrence of liquefaction.

Techniques using the standard penetration test (SPT) have been developed for evaluating soil liquefaction potential (Seed and Idriss 1971, Seed *et al*. 1985, Law *et al*. 1990, Cetin *et al*. 2004, Duman *et al*. 2014). Similarly, methods based on the use of the cone penetration test (CPT) have been developed (Stark and Olson 1995, Robertson and Wride 1998, Juang *et al*. 2003, Moss *et al*. 2006). Other in-situ test methods to evaluate liquefaction potential include the use of the dilatometer (Marchetti 1982) and the shear wave velocity test (Andrus and Stokoe 2000). Statistical methods were commonly adopted to assign probabilities of liquefaction through various statistical classification and regression analyses (Liao *et al*. 1988, Juang *et al*. 1999, Lai *et al*. 2004, Tosun *et al*. 2011).

Finding the liquefaction boundary separating two categories (the occurrence or non-occurrence of liquefaction) for multivariate variables can be considered as a pattern-classification problem. In mathematical terms, an input vector of variables is used to determine a category (classification) by being shown data of known classifications. Some common pattern-recognition tools include discriminant analysis (DA) (Friedman 1989), classification and regression tree (CART) (Breiman *et al*. 1984), neural networks (Specht 1990, Zhang 2000), support vector machine (SVM) (Vapnik *et al*. 1997) and genetic programming (GP) (Muduli and Das 2014a, b, Muduli *et al*. 2014). This study utilizes a modified Multivariate Adaptive Regression Splines (MARS) method (Friedman 1991), in which Logistic Regression (LR) is applied to separate data into various categories.

In this present study, the LR_MARS method was used to analyze three different databases of field liquefaction CPT case records. These three database case records are from Goh (2002), Juang *et al*. (2003) and Chern *et al*. (2008), respectively. Each database is used to train and test the reliability of the LR_MARS model to correctly classify the occurrence or non-occurrence of liquefaction, in comparison with the results from the neural network approaches, including the Probabilistic Neural Network (PNN) model proposed by Goh (2002), a three layer feed-forward network adopted by Juang *et al*. (2003) and a fuzzy-neural system developed by Chern *et al*. (2008). For the neural networks, the training data is used to optimize the connection weights to reduce the errors between the actual and target outputs through minimization of the defined error function (e.g., sum squared error) using the gradient descent approach. Validation of the neural network performance is performed by "testing" with a separate set of data that was never used in training process, to assess the generalization capacity of the trained model to produce the correct input-output mapping even the input is different from the datasets used to train the network. The predictive capacities of neural network models are satisfactory. However, they have been criticized for the computational inefficiency and the poor model interpretability.

2. Elements of analysis

2.1 MARS methodology

Friedman (1991) introduced MARS as a statistical method for fitting the relationship between a set of input variables and dependent variables. MARS is a nonlinear and nonparametric regression method and is based on a divide-and-conquer strategy in which the training data sets are partitioned into separate regions, each gets its own regression line. No specific assumption about the underlying functional relationship between the input variables and the output is required. The end points of the segments are called knots. A knot marks the end of one region of data and the

beginning of another. The resulting piecewise curves, known as basis functions (BFs), give greater flexibility to the model, allowing for bends, thresholds, and other departures from linear functions.

MARS generates BFs by searching in a stepwise manner. It searches over all possible univariate knot locations and across interactions among all variables. An adaptive regression algorithm is used for selecting the knot locations. MARS models are constructed in a two-phase procedure. The forward phase adds functions and finds potential knots to improve the performance, resulting in an overfit model. The backward phase involves pruning the least effective terms. An open MARS source code from Jekabsons (2010) is used in carrying out the analyses presented in this paper.

Let y be the target output and $X = (X_1, ..., X_P)$ be a matrix of P input variables. Then it is assumed that the data are generated from an unknown "true" model. In case of a continuous response this would be

$$y = f(X_1, ..., X_P) + e = f(X) + e \tag{1}$$

in which e is the distribution of the error. MARS approximates the function f by applying basis functions (BFs). BFs are splines (smooth polynomials), including piecewise linear and piecewise cubic functions. For simplicity, only the piecewise linear function is expressed. Piecewise linear functions are of the form $\max(0, x - t)$ with a knot occurring at value t. The equation $\max(.)$ means that only the positive part of $(.)$ is used otherwise it is given a zero value. Formally

$$\max(0, x - t) = \begin{cases} x - t, & \text{if} \quad x \geq t \\ 0, & \text{otherwise} \end{cases} \tag{2}$$

The MARS model $f(X)$, is constructed as a linear combination of BFs and their interactions, and is expressed as

$$f(X) = \beta_0 + \sum_{m=1}^{M} \beta_m \, \lambda_m(X) \tag{3}$$

where each $\lambda_m(X)$ is a basis function. It can be a spline function, or the product of two or more spline functions already contained in the model (higher orders can be used only when the data warrants it; for simplicity, at most second-order is assumed in this paper and the predictive accuracy based on it is proved to be satisfactory). The coefficient β_0 is a constant, and β_m is the coefficient of the mth basis function, estimated using the least-squares method.

Fig. 1 presents a simple example of how MARS would use piecewise linear spline functions to attempt to fit data. The MARS mathematical equation is expressed as

$$\text{Ozone level} = 10.242 - 0.0113 \times \max(0, \text{Wind speed} - 6) \times \max(0, 200 - \text{Visibility}) \tag{4}$$

This expression models air pollution (measured by *ozone level*) as a function of *wind speed* and *visibility*. The term "max" is defined as: max (j, k) is equal to j if $j > k$, else k. The knots are located at *Wind speed* = 6 m/s and *Visibility* = 200 m. Fig. 1 plots the predicted *Ozone level* as *Wind speed* and *Visibility* vary. The figure shows that the *Wind speed* does not affect the *Ozone level* unless the *Visibility* is low. This plot indicates that MARS can build quite flexible regression surfaces by combining knot functions.

The MARS modeling is a data-driven process. To fit the model in Eq. (3), first a forward
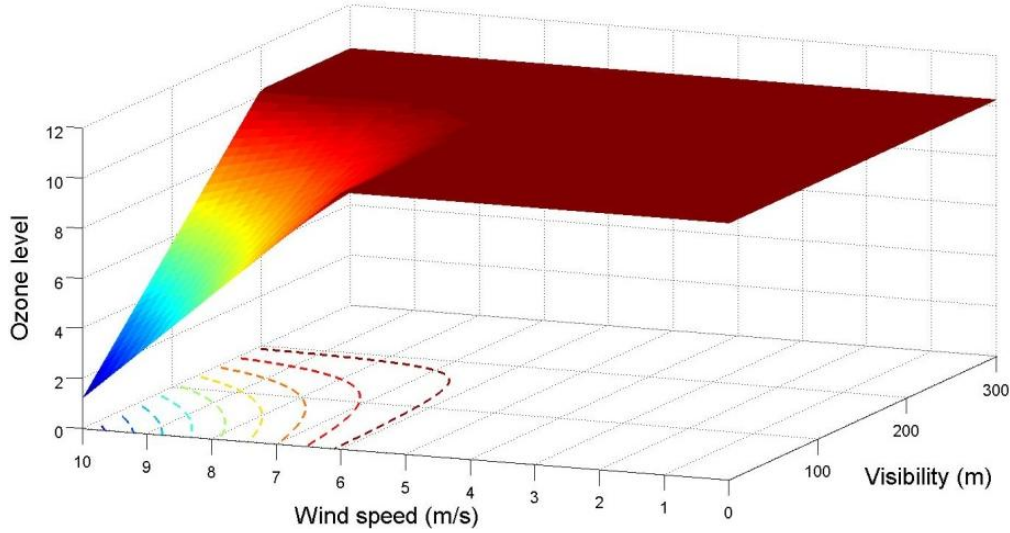
Fig. 1 Knots, linear splines, and variable interaction in a MARS model

selection procedure is performed on the training data. A model is initially constructed with only the intercept β_0, and the basis pair that produces the largest decrease in the training error is added. Considering a current model with M basis functions, the next pair is added to the model in the form

$$\hat{\beta}_{M+1}\lambda_m(X)\max(0, X_j - t) + \hat{\beta}_{M+2}\lambda_m(X)\max(0, t - X_j) \tag{5}$$

with each β being estimated by the method of least squares. As a basis function is added to the model space, interactions between BFs that are already in the model are also considered. BFs are added until the model reaches some maximum specified number of terms K_{max}, leading to a purposely overfit model. K_{max} is set by the user as referenced in Friedman (1991) and generally it is directly related to the number of input parameters n. K_{max} can be assigned any value from $2n$ to n^2.

To reduce the number of terms, a backward deletion sequence follows. The aim of the backward deletion procedure is to find a close to optimal model by removing extraneous variables. The backward pass prunes the model by removing the BFs with the lowest contribution to the model until it finds the best sub-model. Thus, the BFs maintained in the final optimal model are selected from the set of all candidate BFs, used in the forward selection step. Model subsets are compared using the less computationally expensive method of Generalized Cross-Validation (GCV). The GCV equation is a goodness of fit test that penalizes large numbers of BFs and serves to reduce the chance of overfitting. For the training data with N observations, GCV for a model is calculated as follows (Hastie *et al.* 2009)

$$GCV = \frac{\frac{1}{N}\sum_{i=1}^{N}[y_i - f(x_i)]^2}{\left[1 - \frac{M + d \times \frac{M-1}{2}}{N}\right]^2} \tag{6}$$

in which M is the number of BFs, d is the penalizing parameter, representing a cost for each basis function optimization and is a smoothing parameter of the procedure. Larger values for d will lead to fewer knots being placed and thereby smoother function estimates. According to Friedman (1991), the optimal value for d is in the range $2 \leqq d \leqq 4$ and generally the choice of $d = 3$ is fairly effective. In this study, a default value of 3 is assigned to the penalizing parameter d. N is the number of data sets, and $f(x_i)$ denotes the predicted values of the MARS model. The numerator is the mean square error of the evaluated model in the training data, penalized by the denominator. The denominator accounts for the increasing variance in the case of increasing model complexity. Note that $(M - 1)/2$ is the number of hinge function knots. The GCV penalizes not only the number of BFs but also the number of knots. At each deletion step a basis function is removed to minimize Eq. (3), until an adequately fitting model is found. MARS is an adaptive procedure because the selection of BFs and the variable knot locations are data-based and specific to the problem at hand.

After the optimal MARS model is determined, by grouping together all the BFs that involve one variable and another grouping of BFs that involve pairwise interactions (and even higher level interactions when applicable), a procedure termed the analysis of variance (ANOVA) decomposition (Friedman 1991) can be used to assess the relative importance of the contributions from the input variables and the BFs. Previous applications of MARS algorithm in civil engineering can be found in various literatures (Attoh-Okine *et al.* 2009, Lashkari 2012, Mirzahosseinia *et al.* 2011, Zarnani *et al.* 2011, Samui 2011, Samui and Karup 2011, Zhang and Goh 2013, 2014, Goh and Zhang 2014). However, use of MARS in soil liquefaction potential assessment is limited.

2.2 Logistic regression

Linear regression is a commonly used statistical method for predicting values of a dependent variable from observed values of a set of predictor variables. Logistic Regression (LR) is a variation of linear regression for situations where the dependent variable is not a continuous parameter but rather a binary event (e.g., yes/no, good/bad, 0/1). The value predicted by LR is the probability of an event, ranging from 0 to 1. LR is more appropriate than linear regression for assessing seismic liquefaction potential as it allows for binary outputs where each individual liquefaction record is classified as liquefied or non-liquefied (0 for non-liquefied case while 1 for liquefied case). Eq. (1) is applicable for the case of a continuous response of a MARS model. For a binary response, assuming P_r is the estimated probability that an individual case is liquefied, then the LR_MARS model is

$$\text{logit} P_r (y = 1) = f(X_1, \ldots, X_P) + \varepsilon \tag{7}$$

in which the distribution of the error ε is an exponential. Further, Eq. (7) can be expressed as

$$\log\left(\frac{P_r}{1 - P_r}\right) = f(\boldsymbol{X}) = \beta_0 + \sum_{m=1}^{M} \beta_m \, \lambda_m (\boldsymbol{X}) \tag{8}$$

or

$$e^{\log\left(\frac{P_r}{1 - P_r}\right)} = e^{f(\boldsymbol{X})} = e^{\beta_0 + \Sigma_{m=1}^{M} \beta_m \, \lambda_m (\boldsymbol{X})} \tag{9}$$

The estimated liquefaction probability is

Table 1 Confusion matrix

Predicted class	True class	
	Liquefied	Non-liquefied
Liquefied	a	b
Non-liquefied	c	d

$$P_r = \frac{1}{1 + e^{-f(X)}} = \frac{1}{1 + e^{-\beta_0 - \sum_{m=1}^{M} \beta_m \lambda_m(X)}} \qquad (10)$$

in which the β values are estimated using the least-squares method as in Eq. (3).

2.3 Modeling accuracy

Two simple and common methods of evaluating the performance of a pattern-classification model are to determine the error rate (the percentage of misclassified cases, termed as ER) or the success rate (the percentage of correctly classified cases, termed as SR). In assessing the performance of various seismic liquefaction potential models, most researchers have either adopted the success rate or error rate as the criterion.

However, the use of either ER or SR does not take into consideration the misclassification costs (classifying liquefied as non-liquefied and non-liquefied as liquefied) which may not be equal or could be subject to change. When the misclassification costs are not equal, then a confusion matrix is commonly used to quantify the costs and minimize the expected loss. A confusion matrix is a table used to evaluate the performance of a classifier. It is a matrix of the observed versus the predicted classes, with the observed classes in rows and the predicted classes in columns as shown in Table 1.

Table 1 represents a confusion matrix, where each cell contains a count of seismic liquefaction cases belonging to each particular class. There are four classes in total with each cell labeled by a, b, c, and d. The diagonal elements a and d include the frequencies of correctly classified instances and the non-diagonal elements b and c include the frequencies of misclassification. The modeling inaccuracy is easily calculated as $\frac{b+c}{a+b+c+d}$ while the modeling accuracy is expressed as $\frac{a+d}{a+b+c+d}$. Other measures of interest are the proportion of liquefied classified as non-liquefied (termed as Type I error), $\frac{c}{a+c}$, and the proportion of non-liquefied classified as liquefied (termed as Type II error), $\frac{b}{b+d}$. In general, the misclassification costs of liquefaction potential associated with Type I error are higher than those associated with Type II error. It is worse to assess a case as non-liquefied when it is actually liquefied, than it is to assess a case as liquefied when it is in fact non-liquefied.

3. Databases of field liquefaction cases and neural network modeling results

3.1 Database 1

The database used by Juang *et al*. (2003) consists of 226 cases, 133 liquefied cases and 93 non-liquefied. These cases are derived from CPT measurements at over 52 sites and field observations

of 6 different earthquakes. The depths h at which the cases are reported range from 1.4 to 14.1 m. For the details of these cases and the neural network approach, the reader is referred to Juang *et al.* (2003).

The neural network model adopted by Juang *et al.* (2003) utilizes four input neurons representing normalized core penetration resistance q_{c1N}, the soil type index I_c, the effective stress σ'_v and the cyclic stress ratio $CSR_{7.5}$. Among the four inputs, σ'_v is the only variable derived directly from CPT measurements. The q_{c1N}, I_c and $CSR_{7.5}$ are intermediate parameters, determined through the following empirical equations

$$CSR_{7.5} = 0.65 \left(\frac{\sigma_v}{\sigma'_v}\right)\left(\frac{a_{\max}}{g}\right)(r_d)/MSF \qquad \text{(Seed and Idriss 1971)} \qquad (11)$$

$$r_d = \begin{cases} 1.0 - 0.00765z, & if \ z \leqq 9.15 \ m \\ 1.174 - 0.0267z, & 9.15 \ m < z \leqq 23 \ m \end{cases} \qquad \text{(Liao *et al.* 1988)} \qquad (12)$$

$$MSF = 10^{2.24}/M_w^{2.56} = (M_w/7.5)^{-2.56} \qquad \text{(Youd *et al.* 2011)} \qquad (13)$$

$$q_{c1N} = \frac{q_c/100}{(\sigma'_v/100)^{0.5}} \qquad \text{(Robertson and Wride 1998)} \qquad (14)$$

$$I_c = [(3.47 - \log_{10} q_{c1N})^2 + (\log_{10} F + 1.22)^2]^{0.5} \qquad \text{(Robertson 1990)} \qquad (15)$$

$$F = \frac{f_s}{q_c - \sigma_v} \qquad \text{(Robertson 1990)} \qquad (16)$$

where f_s = sleeve friction (kPa); σ_v = total vertical stress (kPa); $a_{\max}$ = the peak acceleration at the ground surface (g); g = acceleration of gravity; r_d = shear stress reduction factor; MSF = magnitude scaling factor; z = depth in meters; M_w = moment magnitude; q_c = measured cone tip resistance (MPa); F = normalized friction ratio. The trained neural network structure and modeling results for the training (tr.) and testing (te.) data are summarized in column 2 of Table 2.

3.2 Database 2

The case records used by Goh (2002) represent 104 sites that liquefied and 66 sites that did not liquefy. PNN approach based on the Bayesian classifier method is used with four layers: the input layer, the pattern layer, the summation layer and the output layer. The inputs consisted of six neurons representing the earthquake magnitude M, $a_{\max}$, σ_v, σ'_v, q_c, and the mean grain size D_{50} (mm). The trained neural network structure and modeling results are summarized in column 3 of Table 2. For the details of these cases and the PNN approach, the reader is referred to Goh (2002).

3.3 Database 3

Database 3 compiled by Chern *et al.* (2008) includes 466 CPT-based field liquefaction records from more than 11 major earthquakes between 1964 and 1999. The records comprised 250 liquefied cases and 216 non-liquefied cases. Chern *et al.* (2008) developed a fuzzy-neural network

Table 2 Summary of CPT databases of field liquefaction cases and neural network modeling results

Database description and neural network modeling results	Database number		
	1	2	3
Observations	226 cases 133 liquefied 93 non-liquefied	170 cases 104 liquefied 66 non-liquefied	466 cases 250 liquefied 216 non-liquefied
Reference	Juang *et al.* (2003)	Goh (2002)	Chern *et al.* (2008)
Neural Network structure	three-layer feed-forward with 3 hidden neurons	four-layer PNN with Bayesian classifier	fuzzy-neural system with 4 clusters and 6 hidden neurons
Data patterns for modeling	151 cases for tr. 75 cases for te.	114 cases for tr. 56 cases for te.	350 cases for tr. 116 cases for te.
Modeling results	SR for tr.: 98% SR for te.: 91% overall SR: 96%	SR for tr.: 100% SR for te.: 100% overall SR: 100%	SR for tr.: 98% SR for te.: 95.7% overall SR: 97.4%
Confusion matrix	96.2% 4.3% 3.8% 95.7%	100% 0% 0% 100%	96.8% 1.9% 3.2% 98.1%

to evaluate the liquefaction potential using 5 parameters: M, σ_v, σ'_v, q_c, and a_{max}. The best trained neural network model and the modeling results are summarized in column 4 of Table 2. In addition, parametric sensitivity analyses indicated that a_{max} and q_c were the two most important parameters influencing liquefaction assessment.

Table 3 LR_MARS models and modeling results

Model	I		II		III	
Database No.	1		2		3	
Input variables	$M\ h\ q_c\ R_f\ \sigma'_v\ \sigma_v\ a_{max}$		$M\ \sigma_v\ \sigma'_v\ q_c\ a_{max}\ D_{50}$		$M\ h\ \sigma_v\ \sigma'_v\ q_c\ a_{max}$	
Data sets for tr. & te.	170 for training 56 for testing		114 for training 56 for testing		350 for training 116 for testing	
Model settings	13 BFs, 2nd order interaction, linear spline		6 BFs, 2nd order interaction, linear spline		12 BFs, 2nd order interaction, linear spline	
Exec. time (s)	0.95		0.17		2.34	
Results plot	Fig. 2		Fig. 3		Fig. 4	
SR	tr.: 94.1% te.: 89.3% overall: 92.9%		tr.: 90.4% te.: 91.1% overall: 90.6%		tr.: 93.4% te.: 87.9% overall: 92.1%	
Confusion matrix	130 (97.7%) 14 (15.1%) 3 (2.3%) 79 (84.9%)		99 (95.2%) 11 (16.7%) 5 (4.8%) 55 (83.3%)		227 (90.8%) 14 (6.5%) 23 (9.2%) 202 (93.5%)	
BFs and model expression	Table 4		Table 5		Table 6	

4. MARS models and modeling results

Three different LR_MARS models were used to analyze the same databases and the results are compared with the neural network results. Table 3 shows the results of LR_MARS models. It summarizes the database used, the input variables, the data sets for training and testing, the model settings, the execution time (PC with 3.0 GHz Intel Core2Quad Q9650 processor, 4 GB RAM), the plot of predictions, the success rates, the confusion matrix and the basis function together with the performance functions for each LR_MARS model. Figs. 2-4 illustrate the training and testing results for LR_MARS models respectively. Tables 4-6 list the corresponding basis functions and LR_MARS expressions for these models. Table 7 shows the ANOVA decomposition of the various LR_MARS models. The relative importance of the input variables and the important
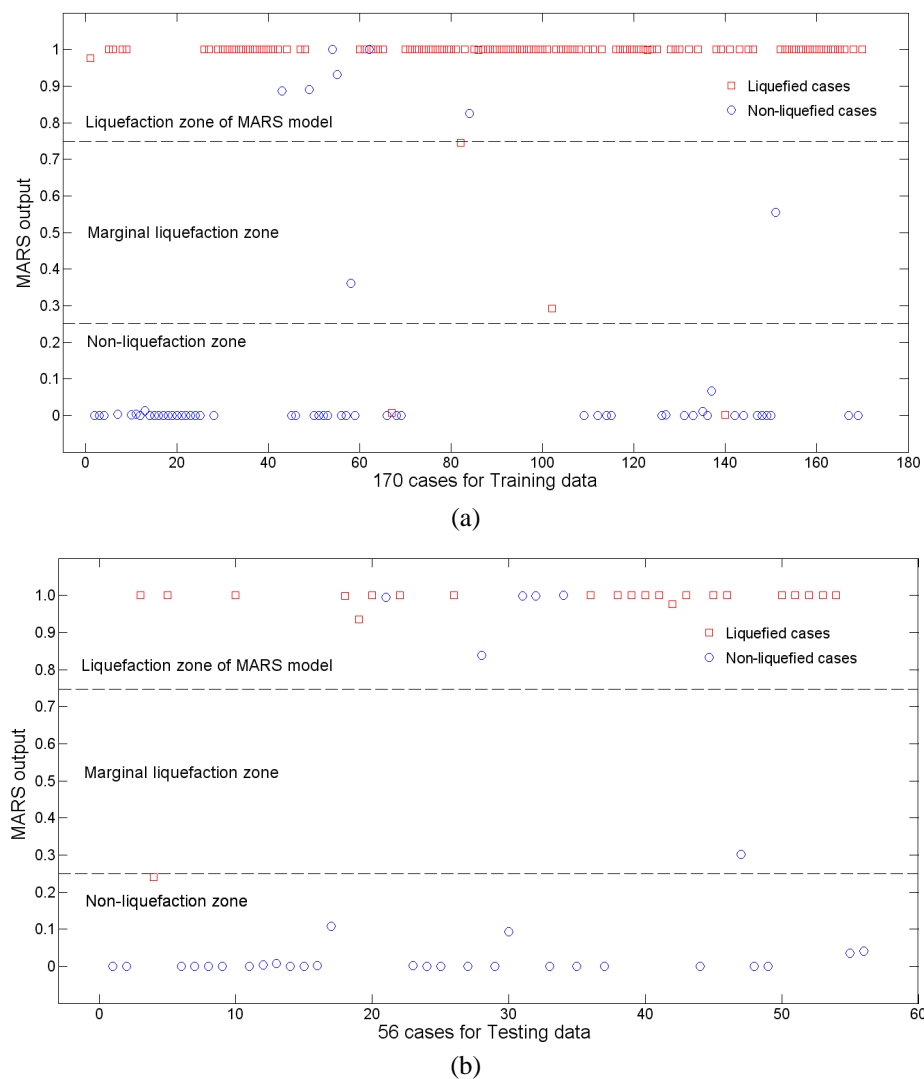

Fig. 2 Modeling results of model I: (a) training data; (b) testing data

Table 4 BFs and LR_MARS expression for model

Basis functions	Expression
BF1	$\max(0, 0.21 - a_{\max})$
BF2	$\max(0, q_c - 3.1)$
BF3	$\max(0, R_f - 2)$
BF4	$BF2 \times \max(0, 5.8 - h)$
BF5	$BF2 \times \max(0, 0.6 - R_f)$
BF6	$BF2 \times \max(0, a_{\max} - 0.15)$
BF7	$BF2 \times \max(0, 0.15 - a_{\max})$
BF8	$BF3 \times \max(0, a_{\max} - 0.19)$
BF9	$BF3 \times \max(0, 0.19 - a_{\max})$
BF10	$BF1 \times \max(0, M - 6.6)$
BF11	$\max(0, R_f - 2.8)$
BF12	$\max(0, h - 4.2)$
BF13	$\max(0, 4.2 - h)$

$y = 26.51 - 372.26 \times BF1 - 5.32 \times BF2 - 40.3 \times BF3 - 0.87 \times BF4 + 6.89 \times BF5 + 11.95 \times BF6$
$\quad + 107.85 \times BF7 + 47.23 \times BF8 + 261.62 \times BF9 + 407.94 \times BF10 + 27.69 \times BF11 - 1.82 \times BF12$
$\quad - 5.13 \times BF13$

$$f(x) = \frac{1}{1 + e^{-y}}$$

interaction terms between input parameters for each LR_MARS model are also shown in Table 7.

4.1 Model I

Model I is the LR_MARS model used to analyze database 1 which consisted of 170 training and 56 testing records. The input variables were M, h, q_c, R_f, σ'_v, σ_v and $a_{\max}$. The training and testing results are shown in Fig. 2. Model I has an overall success rate of 92.5%. The model accuracy in predicting liquefied cases is very high (97.7%). The Type I error is very low (2.3%). Table 4 shows the basis function expressions and Model I expression. The derived $f(x)$ can be used to determine the liquefaction potential. ANOVA decomposition of model I in row 2 of Table 7 indicates that q_c and $a_{\max}$ are the two most significant parameters. The ANOVA decomposition also indicates that interaction between q_c and $a_{\max}$ is significant.

4.2 Model II

Model II is the LR_MARS model used to analyze database 2 which consisted of 114 training and 56 testing records. The input variables were M, σ_v, σ'_v, q_c, $a_{\max}$ and D_{50}. The training and testing results are shown in Fig. 3. Model II has an overall success rate of 90.6%. The model accuracy in predicting liquefied cases is relatively high (95.2%). The Type I error is 4.8%. Table 5 shows the basis function expressions and model II expression. ANOVA decomposition of model II in row 3 of Table 7 indicates that q_c and M are the two most significant parameters. The interaction between M and σ_v is also of significance in assessing liquefaction potential.
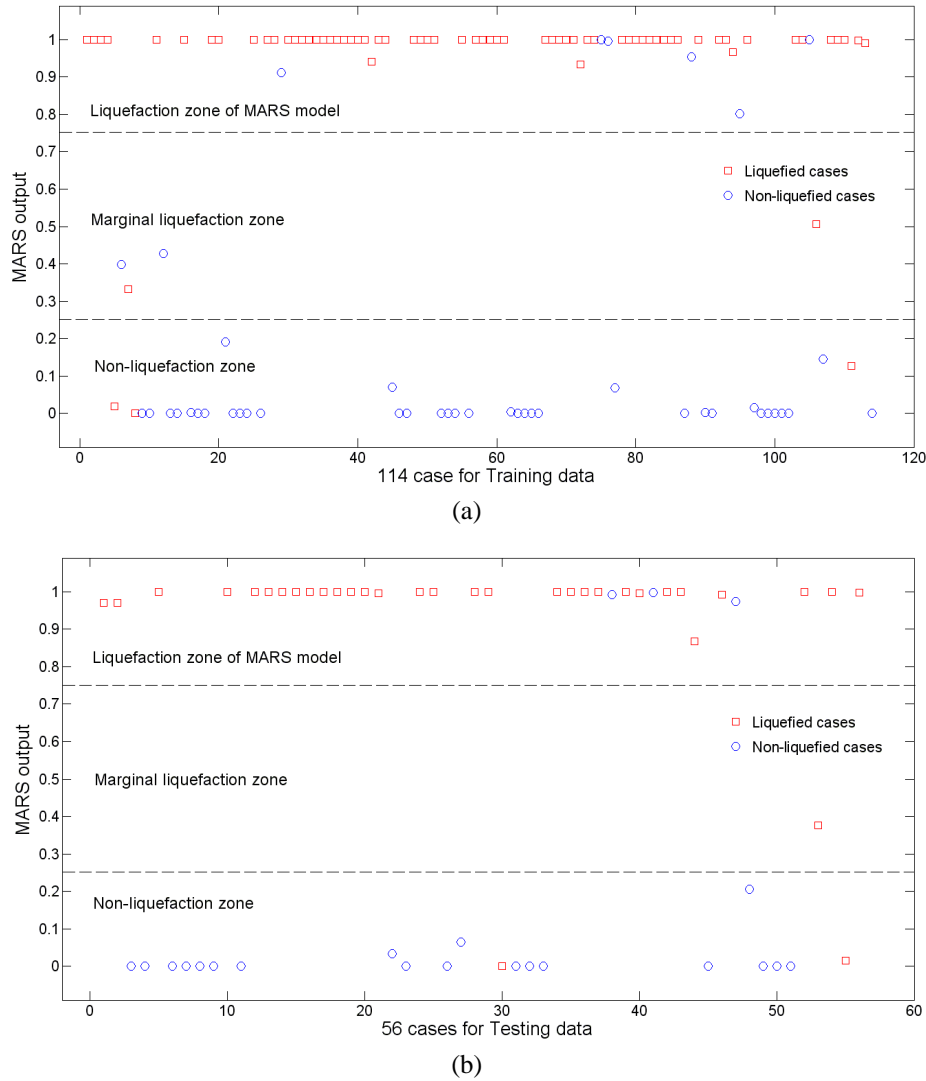
Fig. 3 Modeling results of model II: (a) training data; (b) testing data

4.3 Model III

Model III is the LR_MARS model used to analyze database 3 which consisted of 350 training and 116 testing patterns. The input variables include M, h, σ_v, σ'_v, q_c, and a_{max}. The training and testing results are shown in Fig. 4. Model III has an overall success rate of 92.1%. The model accuracy in predicting liquefied cases is 90.8% and in predicting non-liquefied cases is 93.5%. The Type I error is 9.2%. Table 6 shows the basis function expressions and model III expression. ANOVA decomposition of model III in row 4 of Table 6 indicates that q_c and a_{max} are the two most significant parameters, which are consistent with the conclusions of Chern *et al*. (2008). The interaction between q_c and a_{max} is also of significance.

Table 5 BFs and LR_MARS expression for model

Basis functions	Expression
BF1	$\max(0, 13.85 - q_c)$
BF2	$BF1 \times \max(0, 0.16 - a_{max})$
BF3	$\max(0, M - 6.4)$
BF4	$\max(0, 6.4 - M)$
BF5	$BF3 \times \max(0, 215.7 - \sigma_v)$
BF6	$BF1 \times \max(0, \sigma_v - 153)$

$$f(x) = \frac{1}{1 + e^{-(-22.65 + 3.44 \times BF1 - 72.35 \times BF2 + 13.46 \times BF3 - 32.19 \times BF4 - 0.07 \times BF5 - 0.04 \times BF6)}}$$
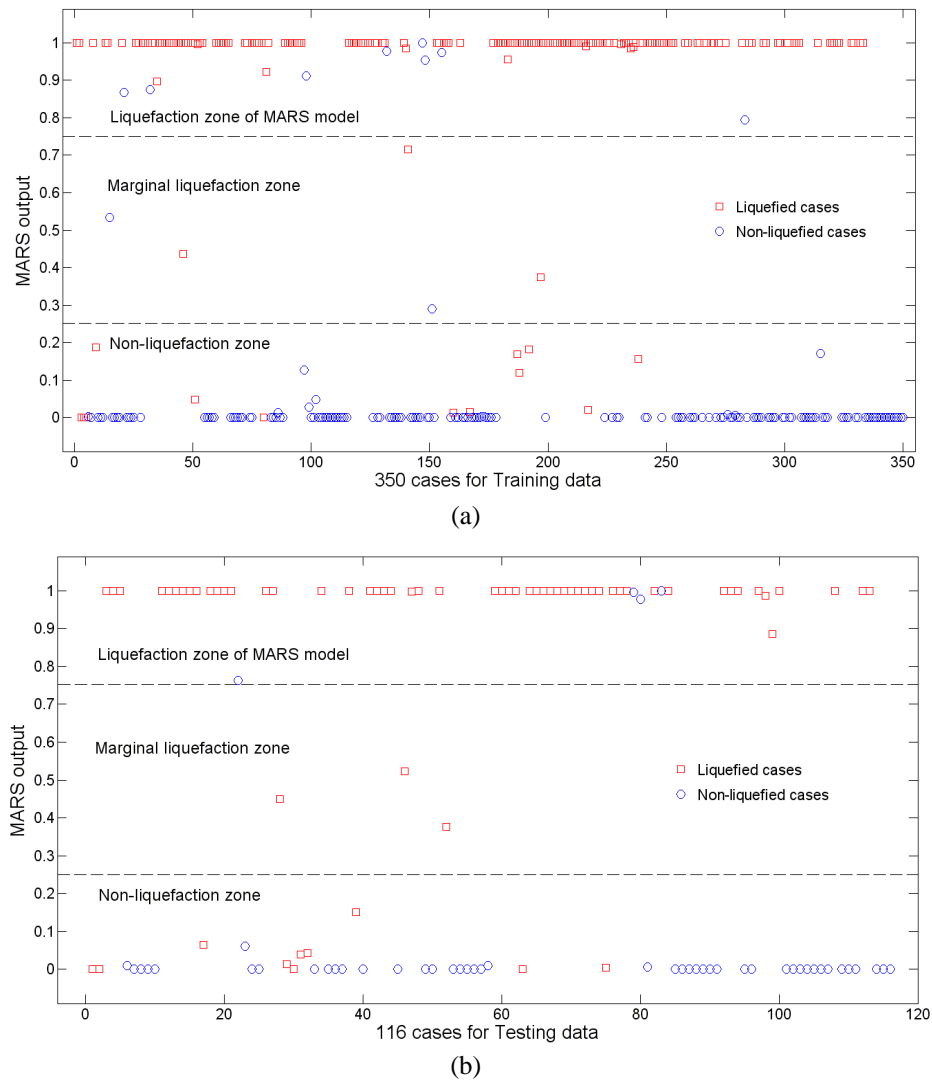

(a)

(b)

Fig. 4 Modeling results of model III: (a) training data; (b) testing data

Table 6 BFs and LR_MARS expression for model

Basis functions	Expression
BF1	$\max(0, 10.61 - q_c)$
BF2	$\max(0, 0.22 - a_{max})$
BF3	$BF1 \times \max(0, \sigma_v - 136.8)$
BF4	$\max(0, M - 6)$
BF5	$\max(0, 6 - M)$
BF6	$\max(0, a_{max} - 0.22) \times \max(0, 5.5 - q_c)$
BF7	$BF1 \times \max(0, a_{max} - 0.25)$
BF8	$BF1 \times \max(0, 0.25 - a_{max})$
BF9	$BF2 \times \max(0, \sigma'_v - 59.8)$
BF10	$BF2 \times \max(0, 59.8 - \sigma'_v)$
BF11	$\max(0, q_c - 5.8)$
BF12	$\max(0, 5.8 - h)$

$$y = -17.71 + 5.48 \times BF1 - 187.87 \times BF2 - 0.04 \times BF3 + 5.65 \times BF4 - 202.65 \times BF5 - 27.72 \times BF6$$
$$+9.23 \times BF7 - 22.17 \times BF8 + 3.41 \times BF9 + 12.28 \times BF10 - 1.46 \times BF11 - 2.89 \times BF12$$

$$f(x) = \frac{1}{1 + e^{-y}}$$

Table 7 Parameters derived from ANOVA decomposition for each model

Model	The two most important single variables	The most important interaction terms
I	q_c & a_{max}	(q_c, a_{max})
II	q_c & M	(M, σ_v)
III	q_c & a_{max}	(q_c, a_{max})

4.4 ANOVA decomposition

As described previously, ANOVA decomposition was used to assess the contributions from the input variables and the interaction between the various input parameters. Table 7 displays the ANOVA decomposition of the three LR_MARS models. For each model, the two most significant (important) single variables in determining model accuracy are listed. Also listed are the most important interaction factors between earthquake parameters (M and a_{max}), in situ stress factors (σ_v and σ'_v) and the soil resistance factors (q_c).

5. Conclusions

This paper has demonstrated the usefulness of the LR_MARS approach to model the complex relationship between the seismic parameters, the in situ stress factors, the soil resistance factors and the liquefaction potential using the in situ measurements based on the CPT field tests. Comparisons indicate that the LR_MARS performs as well as, or marginally worse than, neural network methods in terms of accuracy. However, considering its computational efficiency, simplicity of interpretation, predictive accuracy, its data-driven and adaptive nature, its ability to

map the interaction between variables and the relatively low number of Type I error predictions, the use of LR_MARS model in assessing seismic liquefaction potential is promising. Since MARS explicitly defines the intervals (boundaries) for the input variables, the model enables engineers to have an insight and understanding of where significant changes in the data may occur.

It should be noted that the performance of MARS deteriorates significantly when small or scarce sample sets are used. As the built MARS model makes predictions based on the knot values and the basis functions, interpolations between the knots of design variables are more accurate and reliable than extrapolations. The proposed LR_MARS models was developed using database records with limited ranges of earthquake parameters, soil properties, and in situ stress factors. Therefore it is not recommended that the model be applied for values of input parameters beyond the specified ranges in this study. Additional new data sets are required to further evaluate and update the current LR_MARS models.

Acknowledgments

References

Andrus, R.D. and Stokoe, K.H. (2000), "Liquefaction resistance of soils from shear-wave velocity", *J. Geotech. Geoenviron*., **126**(11), 1015-1025.

Atign, E. and Byrne, P.M. (2004), "Liquefaction flow of submarine slopes under partially undrained conditions: an effective stress approach", *Can. Geotech. J*., **41**(1), 154-165.

Attoh-Okine, N.O., Cooger, K. and Mensah, S. (2009), "Multivariate adaptive regression spline (MARS) and hinged hyper planes (HHP) for doweled pavement performance modeling", *Constr. Build. Mater*., **23**(9), 3020-3023.

Breiman, L., Friedman, J.H., Olshen, R.A. and Stone, C.J. (1984), *Classification and Regression Trees*, Wadsworth & Brooks, Monterey, CA, USA.

Cetin, K.O., Seed, R.B., Der Kiureghian, A.K., Tokimatsu, K., Harder, L.F. Jr., Kayen, R.E. and Moss, R.E.S. (2004), "Standard penetration test-based probabilistic and deterministic assessment of seismic soil liquefaction potential", *J. Geotech. Geoenviron*., **130**(12), 1314-1340.

Chen, Y., Liu, H. and Wu, H. (2013), "Laboratory study on flow characteristic of liquefied and post-liquefied sand", *Eur. J. Environ. Civil Eng*., **17**, 23-32.

Chen, Y., Xu, C., Liu, H. and Zhang, W. (2015), "Physical modeling of lateral spreading induced by inclined sandy foundation in the state of zero effective stress", *Soil Dyn. Earthq. Eng*., **76**, 80-85.

Chern, S.G., Lee, C.Y. and Wang, C.C. (2008), "CPT-based liquefaction assessment by using fuzzy-neural network", *J. Mar. Sci. Technol*., **16**(2), 139-148.

Duman, E.S., Ikizier, S.B., Angin, Z. and Demir, G. (2014), "Assessment of liquefaction potential of the Erzincan, Eastern Turkey", *Geomech. Eng*., *Int. J*., **7**(6), 589-612.

Friedman, J.H. (1989), "Regularized discriminant analysis", *J. Am. Stat. Assoc*., **84**(405), 165-175.

Friedman, J.H. (1991), "Multivariate adaptive regression splines", *Ann. Stat*.,**19**, 1-141.

Goh, A.T.C. (2002), "Probabilistic neural network for evaluating seismic liquefaction potential", *Can. Geotech. J*., **39**(1), 219-232.

Goh, A.T.C. and Zhang, W.G. (2014), "An improvement to MLR model for predicting liquefaction-induced lateral spread using multivariate adaptive regression splines", *Eng. Geol*., **170**, 1-10.

Hastie, T., Tibshirani, R. and Friedman, J. (2009), *The Elements of Statistical Learning*: *Data Mining*,

Inference and Prediction, (2nd Edition), Springer-Verlag, New York, NY, USA.

Jekabsons, G. (2010), *VariReg*: *A Software Tool for Regression Modelling using Various Modeling Methods*, Riga Technical University, Latvia. URL: http://www.cs.rtu.lv/jekabsons/

Juang, C.H., Rosowsky, D.V. and Tang, W.H. (1999), "Reliability-based method for assessing liquefaction potential of soils", *J. Geotech. Geoenviron.*, **125**(8), 684-689.

Juang, C.H., Yuan, H., Lee, D.H. and Lin, P.S. (2003), "Simplified cone penetration test-based method for evaluating liquefaction resistance of soils", *J. Geotech. Geoenviron.*, **129**(1), 66-80.

Lade, P.V. and Yamamuro, J.A. (2011), "Evaluation of static liquefacion potential of silty sand slopes", *Can. Geotech. J.*, **48**(2), 247-264.

Lai, S.Y., Hsu, S.C. and Hsieh, M.J. (2004), "Discriminant model for evaluating soil liquefaction potential using cone penetration test data", *J. Geotech. Geoenviron.*, **130**(12), 1271-1282.

Lancelot, L., Shahrour, I. and Mahmoud, M.A. (2004), "Instability and static liquefaction on proportional strain paths for sand at low stresses", *J. Eng. Mech.*, **130**(11), 1365-1372.

Lashkari, A. (2012), "Prediction of the shaft resistance of non-displacement piles in sand", *Int. J. Numer. Anal. Met.*, **38**(7), 904-931.

Law, K.T., Cao, Y.L. and He, G.N. (1990), "An energy approach for assessing seismic liquefaction potential", *Can. Geotech. J.*, **27**(3), 320-329.

Liao, S.C., Veneziano, D. and Whitman, R.V. (1988), "Regression models for evaluating liquefaction probability", *J. Geotech. Eng.*, **114**(4), 389-411.

Liu, H., Chen, Y.M., Yu, T. and Yang, G. (2014), "Seismic analysis of the Zipingpu concrete-faced rockfill dam response to the 2008 Wenchuan, China, Earthquake", *J. Perform. Constr. Facil.*, **29**(5), 0401429. DOI: 10.1061/(ASCE)CF.1943-5509.0000506

Marchetti, S. (1982), "Detection of liquefiable sand layers by means of quasi-static penetration tests", *Proceedings of the 2nd European Symposium on Penetration Testing*, Volume 2, Amsterdam, The Netherlands, May, pp. 458-482.

Mirzahosseini, M., Aghaeifar, A., Alavi, A., Gandomi, A. and Seyednour, R. (2011), "Permanent deformation analysis of asphalt mixtures using soft computing techniques", *Expert. Syst. Appl.*, **38**(5), 6081-6100.

Moss, R.E.S., Seed, R.B., Kayen, R.E., Stewart, J.P., Der Kiureghian, A.K. and Cetin, K.O. (2006), "CPT-based probabilistic and deterministic assessment of in situ seismic soil liquefaction potential", *J. Geotech. Geoenviron.*, **132**(8), 1032-1051.

Muduli, P.K. and Das, S.K. (2014a), "CPT-based seismic liquefaction potential evaluation using multi-gene genetic programming approach", *Ind. Geotech. J.*, **44**(1), 86-93.

Muduli, P.K. and Das, S.K. (2014b), "Evaluation of liquefaction potential of soil based on standard penetration test using multi-gene genetic programming model", *Acta. Geophys.*, **62**(3), 529-543.

Muduli, P.K., Das, S.K. and Bhattacharya, S. (2014), "CTP-based probabilistic evaluation of seismic soil liquefaction potential using multi-gene genetic programming", *Georisk*, **8**(1), 14-28.

Robertson, P.K. (1990), "Soil classification using the cone penetration test", *Can. Geotech. J.*, **27**(1), 151-158.

Robertson, P.K. and Wride, C.E. (1998), "Evaluating cyclic liquefaction potential using the cone penetration test", *Can. Geotech. J.*, **35**(3), 442-459.

Samui, P. (2011), "Determination of ultimate capacity of driven piles in cohesionless soil: A multivariate adaptive regression spline approach", *Int. J. Numer. Anal. Method. Geomech.*, **36**(11), 1434-1439.

Samui, P. and Karup, P. (2011), "Multivariate adaptive regression spline and least square support vector machine for prediction of undrained shear strength of clay", *Int. J. Appl. Metaheur. Comput.*, **3**(2), 33-42.

Seed, H.B. and Idriss, I.M. (1971), "Simplified procedure for evaluating soil liquefaction potential", *Soil Mech. Found. Eng.*, **97**(9), 1249-1273.

Seed, H.B., Tokimatsu, K., Harder, L.F. and Chung, R. (1985), "Influence of SPT procedures in soil liquefaction resistance evaluations", *J. Geotech. Eng.*, **111**(12), 861-878.

Specht, D. (1990), "Porbabilistic neural networks", *Neural Networks*, **3**(1), 109-118.

Stark, T.D. and Olson, S.M. (1995), "Liquefaction resistance using CPT and field case histories", *J. Geotech. Eng.*, **121**(12), 856-869.

Tosun, H., Seyrek, E., Orhan, A., Savas, H. and Turkoz, M. (2011), "Soil liquefaction potential in Eskisehir,

NW Turkey", *Nat. Hazard Earth Syst.*, **11**, 1071-1082.

Toyota, H., Towhata, I., Imamura, S. and Kudo, K. (2004), "Shaking table tests on flow dynamics in liquefied slope", *Soils Found.*, **44**(5), 67-84.

Vapnik, V., Golowich, S. and Smola, A. (1997), "Support vector method for function approximation, regression estimation, and signal processing", *Adv. Neural Inform. Process. Syst.*, **9**, 281-287.

Youd, T.L., Idriss, I., Andrus, R., Arango, I., Castro, G., Christian, J., Dobry, R., Finn, W., Harder, L. Jr., Hynes, M., Ishihara, K., Koester, J., Liao, S., Marcuson, W. III, Martin, G., Mitchell, J., Moriwaki, Y., Power, M., Robertson, P., Seed, R. and Stokoe, K. II (2001), "Liquefaction resistance of soils: Summary report from the 1996 NCEER and 1998 NCEER/NSF workshops on evaluation of liquefaction resistance of soils", *J. Geotech. Geoenviron.*, **127**(10), 817-833.

Zarnani, S., El-Emam, M. and Bathurst, R.J. (2011), "Comparison of numerical and analytical solutions for reinforced soil wall shaking table tests", *Geomech. Eng., Int. J.*, **3**(4), 291-321.

Zhang, G.Q. (2000), "Neural networks for classification: A survey", *IEEE Transactions on Systems*, *Man*, *and Cybernetics-Part C*: *Applications and Reviews*, **30**(4), 451-462.

Zhang, W.G. and Goh, A.T.C. (2013), "Multivariate adaptive regression splines for analysis of geotechnical engineering systems", *Comput. Geotech.*, **48**, 82-95.

Zhang, W.G. and Goh, A.T.C. (2014), "Multivariate adaptive regression splines model for reliability assessment of serviceability limit state of twin caverns", *Geomech. Eng., Int. J.*, **7**(4), 431-458.

CC